Available online at www.sciencedirect.com
ScienceDirect
Organic Electronics 9 (2008) 262–266
Organic Electronics
www.elsevier.com/locate/orgel

Letter

Improved performance in n-channel organic thin film transistors by nanoscale interface modification

Chih-Wei Chu [a,b,*], Chao-Feng Sung [c], Yuh-Zheng Lee [c], Kevin Cheng [c]

[a] Research Center for Applied Sciences, Academia Sinica, Taipei 11529, Taiwan
[b] Department of Photonics, National Chiao-Tung University, Hsinchu 300, Taiwan
[c] Industrial Technology Research Institute, Hsinchu 300, Taiwan

Received 16 July 2007; received in revised form 22 November 2007; accepted 27 November 2007
Available online 26 December 2007

Abstract

We demonstrate that the electrical properties of n-channel thin film transistors can be enhanced by inserting a nanoscale interfacial layer, namely, cesium carbonate (Cs_2CO_3), between organic semiconductor and source/drain electrodes. Devices with the Cs_2CO_3/Al electrode showed a reduction of contact resistance, not only with respect to Al, but also compared to Ca. The improvement is attributed to the reduction in the energy barrier of electron injection and the prevention of unfavorable chemical interaction between the organic layer and the metal electrode. High field-effect mobility of 0.045 cm^2/V s and on/off current ratios of 10^6 were obtained in the [6,6]-phenyl C60 butyric acid methyl ester-based organic thin film transistors using the Cs_2CO_3/Al electrodes at a gate bias of 40 V.

PACS: 73.40.Cg

Keywords: n-Type; Organic thin film transistors; Nanoscale interface modification

In recent years, there has been a worldwide interest in developing organic thin film transistors (OTFTs) due to their potential application in display drivers, radio frequency identification tags, and smart cards [1–3]. Great progress has been achieved so far in p-type OTFTs, whose electronic properties have already reached the level of hydrogenated amorphous silicon (a-Si:H). For example, field effect mobilities greater than 1 cm^2/V s and high on/off current ratio ($>10^6$) have been obtained in pentacene-TFTs [4]. However, the development of n-type OTFTs with comparable performance remains a key issue in terms of meeting the requirements for practical applications. Although a large number of studies have focused on improving the intrinsic electrical properties of n-type materials [5,6] and their applications, [7,8] devices still exhibit limited life span. This could be attributed to the instability of single component π-electron materials, which can easily undergo surface oxidation/deoxidation and chemical interaction with metal electrodes. Moreover, low work function metals, used to reduce energy barriers and promote electron injection [9,10], are diffi-

* Corresponding author. Address: Research Center for Applied Sciences, Academia Sinica, Taipei 11529, Taiwan. Tel.: +886 2 2789 8000.
E-mail address: gchu@gate.sinica.edu.tw (C.-W. Chu).

1566-1199/$ - see front matter © 2007 Elsevier B.V. All rights reserved.
doi:10.1016/j.orgel.2007.11.008

cult to process because of their susceptibility to atmospheric moisture and oxygen. These factors henceforth indicate that the property of organic–metal electrode interface play an important role in obtaining high performance n-type OTFTs; however, engineering of the interface has not received much attention in n-type OTFTs [11].

An alternative approach for replacing the reactive metal as an electrode is to insert a thin layer of alkali metal halides [12] and carboxylates [13], in various attempts at improving the charge injection from an Al cathode to an emitting layer for organic light emitting diodes (OLED). Similarly, the source/drain (S/D) contacts in the OTFTs have significant influence on device operation. For example, their contribution to the contact resistance arise from mismatching work functions, and/or interaction between the metal electrodes and the organic semiconductor [14,15]. Recently, it has been reported that Cs_2CO_3 is one of the best electron injection materials among a wide range of metal electrodes, and can be used as an electron injection layer for OLED by thermal and solution deposition [13,16]. In this letter, we present the conclusion that the performance of the [6,6]-phenyl C60 butyric acid methyl ester (PCBM)-based n-type OTFTs with an bi-layer S/D electrodes is greatly improved over the bare Al, and calcium electrodes. The performance enhancement of our devices is achieved by using a nanoscale interfacial modification layer made of Cs_2CO_3. The presence of a Cs_2CO_3 layer at the organic/Al interface significantly reduces the contact barrier and provides protection against diffusion and chemical interaction between organic layer and metal electrodes.

The devices were fabricated on ITO-coated glass substrates (10–20 Ω/sq sheet resistance). ITO-coated glass substrate was used as the gate electrode. After routine solvent cleaning, the substrates were treated with UV-ozone for 15 min. The cleaned ITO substrates were then covered with 750-nm-thick polymer dielectric insulator, prepared by spin-coating a solution of poly-4-vinylphenol (11 wt%) and poly(melamineco-formaldehyde) (4 wt%) in propylene glycol monomethyl ether acetate (PGMEA). The substrate was then prebaked at 100 °C for 5 min, followed by baking at 200 °C for 20 min, to cross-link the polymer. The thickness of the PVP films was 680 nm. The resulting capacitance per unit area of the film, C_i, was 5.47 nF/cm^2. The semiconductor layer, consisting of a 50-nm-thick layer of PCBM (purchased from Solenne B.V.), was spun over the cross-linked PVP from a 1 wt% ratio chloroform solution in a nitrogen environment inside a glove box. Prior to S/D electrode deposition, the device was thermally annealed on a hot plate at 70 °C for a period of 20 min. Finally, Cs_2CO_3 (Sigma–Aldrich, 99% purity) was deposited by a Knudsen cell (k-cell), a molecular beam epitaxy single-filament effusion cell from Veeco/Applied Epi, and Al was thermally evaporated onto the PCBM film through a shadow mask to form the S/D electrodes. The thicknesses of Cs_2CO_3 and Al films were 1 nm and 80 nm, respectively. A schematic cross-section of our top-contact OTFTs is presented in the inset of Fig. 1a with a channel length of 170 μm and width of 2 mm. For comparison, Ca, Al, and Au were investigated as alternative to the Cs_2CO_3/Al as S/D contacts. All thermal evaporations were done under a pressure of less than

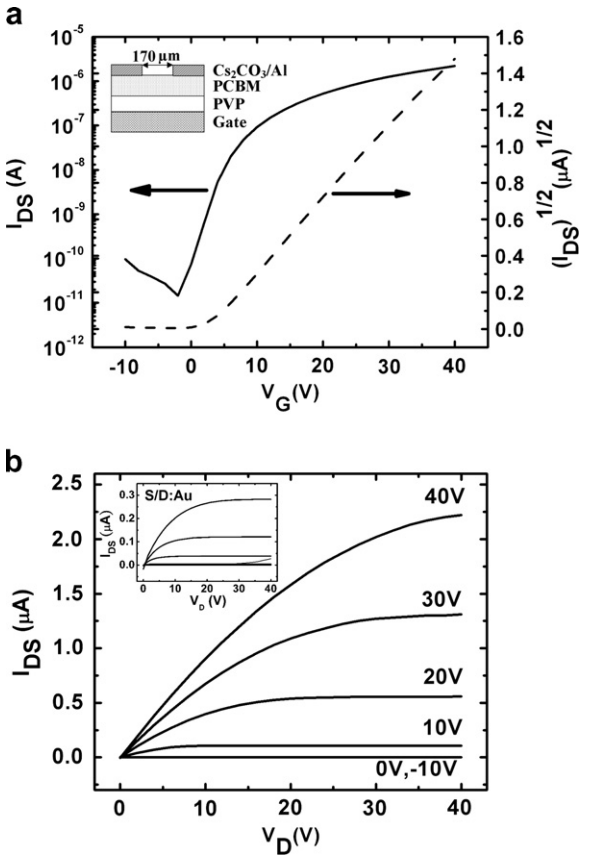

Fig. 1. (a) Typical transfer characteristics of the OTFT with Cs_2CO_3/Al electrodes at a constant drain voltage of 40 V. Inset: schematic structure of a top-contact OTFT. (b) Source/drain current–voltage characteristics of the OTFT with Cs_2CO_3/Al electrodes. Inset: source/drain current–voltage characteristics of the OTFT with Au electrode.

6×10^{-6} torr and the film thickness was monitored with a quartz oscillator. The electrical measurements of the devices were performed in a nitrogen environment inside a glove box using a Keithley 4200 semiconductor parameter analyzer and HP 4980A Precision LCR meter.

Typical transfer and output curve characteristics of the PCBM OTFTs, with Cs_2CO_3/Al S/D electrodes, are shown in Fig. 1a and b, respectively. The device exhibited typical n-channel characteristics with good linear/saturation behavior, without any apparent negative drain current resulting from gate leakage at $V_{DS} = 0$ V and significant low gate leakage ($<4 \times 10^{-9}$ A) even at $V_G = 40$ V. Strong field-effect modulation of the channel conductance was observed, with on/off current ratios (I_{on}/I_{off}) as high as 10^6 (measured between gate voltage, $V_G = -10$–40). The field-effect mobility (μ) and threshold voltage (V_T) were extracted from the measured transfer curve by comparing it with the standard transistor's current–voltage equation in the saturation regime: $I_{DS,sat} = (WC_i/2L)\mu(V_G - V_T)$ [2,17] where $I_{DS,sat}$ is the saturated drain current. The μ and the V_T of the OTFT were found to be 4.45×10^{-2} cm^2/V s and -2.3 V, respectively.

It has been proposed that PCBM has much lower electron affinity compared to C_{60} [18]. In addition, the energy level of lowest occupied molecular orbital (LUMO) for PCBM is 3.7 eV [19]. Therefore, the electron injection current can be limited by the selection of electrode materials. As shown in the idealized transfer characteristics for different materials for the S/D electrodes, Fig. 2, the slope for Cs_2CO_3/Al devices results in higher μ and lower V_T, not only with respect to Al ($\Phi = 4.1$ eV), but also compared to Ca ($\Phi = 2.8$ eV). The device with Ca and Al electrodes had similar I_{on}/I_{off} compared to the device with Cs_2CO_3/Al electrode, while the decreased slope of the transfer characteristics corresponded to the decrease in field-effect mobilities. For further demonstrated the electron current is contact-limited. We have fabricated the devices with Au ($\Phi = 5.0$ eV) as S/D electrodes. The output curve characteristic for the PCBM OTFTs with Au is shown in the inset of Fig. 1b. Due to the large energy level mismatch between Au work function and LUMO level of PCBM, the injection of electrons from Au to PCBM is a difficult process. The mobility for the PCBM OTFTs with Au was determined from the transfer curve characteristics (saturation region) to be 0.0081, which is smaller by quintuple of magnitude than that of the PCBM OTFTs with Cs_2CO_3/Al as electrodes. Thus, the increase of the field effect mobilities with decreasing work-function suggests that the contact effect lowers the extrinsic field-effect mobility than the intrinsic value. The summary of parameters for the devices made in this study is given in Table 1.

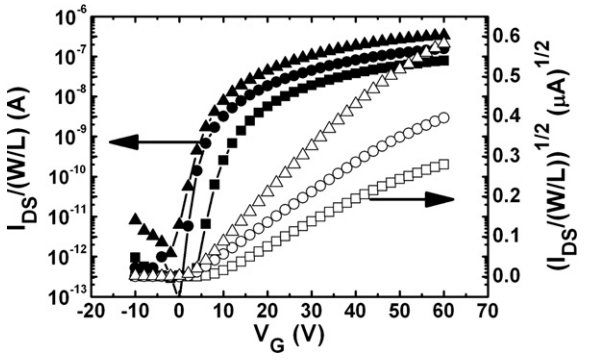

Fig. 2. Idealized I_{SD}–V_G (solid) and $(I_{SD})^{1/2}$–V_G (open) plots for different materials as the source/drain contacts at V_D=40 V. Cs_2CO_3/Al (triangles); Ca/Al (circle); Al (square).

Although the work-function of Ca is lower than the LUMO level of PCBM, with no energy barrier, and with a thin layer Cs_2CO_3 between PCBM and electrode, mobility is more than doubled compared to that obtained with the Ca electrodes. It was reported that the lowering of the vacuum level of organic semiconductors was observed with a thin layer of Cs_2CO_3 by an ultraviolet photoelectron spectrometer [20,21]. The energy offset between the Fermi level of the electrode and the LUMO of semiconductors at interface is greatly reduced. Therefore, the improvement of the device performance is attributed to Cs_2CO_3 lowering the barrier for electron injection from Al to the LUMO level of PCBM. Moreover, earlier studies on Cs_2CO_3 indicated that Cs_2CO_3 decomposes into cesium oxide during thermal evaporation [22]. With a metal oxide as a buffer layer, it will consume most of the interface of metal and leave the

Table 1
Summary of the performance of the PCBM OTFTs with different source/drain electrodes materials

S/D electrode	μ (cm^2/V^{-1} s)	V_t (V)	S (V/decade)	On/off ratio
Au	0.0081	4.87	1.81	10^3
Al	0.0120	3.15	1.80	10^6
Ca/Al	0.0227	0.74	1.45	10^6
Cs_2CO_3/Al	0.0445	−2.30	1.39	10^6

The values are an average of ten different devices with practical standard deviation.

organic semiconductor intact [23]; therefore, Cs_2O could serve as a protective agent for PCBM against metal-induced degradation and a better interface (absence of reactive Ca), hence further minimizing contact resistance. Fig. 3 shows the contact resistance (R_C), obtained according to the method in Ref. [24], (extracted at $|V_{SD}| = 4$ V and in linear regime) as a function of the V_G with different materials as S/D electrodes. The R_C of Ca electrode decreased from 8×10^8 to 3×10^8 Ω as V_G varied from 10 to 40 V. In contrast, the R_C of Cs_2CO_3/Al electrode was insensitive with V_G, and is decreased more than twofold compared to the Ca electrode. The change of potential drop at the organic–metal electrode interface due to the variation of R_C will change the distribution of the electric field in the vertical direction, which influences the V_T (the higher the contact resistance, the larger the V_T) [25]. Hence the decrease of R_C due to the introduction of the Cs_2CO_3 in our OTFTs will lead to the reduction of V_T, as can be seen in Table 1. This result demonstrates that the introduction of the Cs_2CO_3 in our OTFTs played an important role in the enhancement of the device performance.

Recently, Li et al. reported that Cs_2CO_3 is decomposed to metallic Cs during thermal evaporation, as measured with the quartz crystal microbalance [26]. However, contrary to the observation of Li et al., we found that the 230-nm-thick Cs_2CO_3 film has a capacitance of about 6.9 nF/cm^2 at 1 kHz with good insulator properties. In addition, the pressure in the vacuum chamber had increased rapidly as the k-cell temperature raised above 690 °C which we believe was due to the formation of Cs_2O and CO_2 [23,27]. Since Cs_2CO_3 layer was deposited by thermal evaporation, the small amount of metallic Cs might also be introduced into the film during thermal evaporation. However, the proportion of the Cs within the composite film is quite low, and Cs would absorb the residual oxygen in vacuum to form Cs_2O; the electrical conductivity of the composite film is still in the insulating region. Hence, as-deposited Cs_2CO_3 film is a dielectric with good insulating properties. With the presence of a thin Cs_2CO_3 layer, the energy barrier for electrons from Al to PCBM could be greatly lowered by the larger potential drop, resulting in increasing the injection of electrons via tunneling. As the Cs_2CO_3 becomes thicker, it leads to slowing down of tunneling probability. As can be seen in Fig. 4, the transfer characteristics of the devices are dependent on the thickness of Cs_2CO_3 layer. The device with 1 nm thick Cs_2CO_3 exhibits the highest mobility. With the further incremental thickness of Cs_2CO_3 layer, mobility has gradually decreased.

In conclusion, we have demonstrated that the performance of PCBM-based n-channel OTFTs can be improved by inserting a thin Cs_2CO_3 film between the PCBM and S/D electrode. The current and the field-effect mobility were significantly improved, when compared to Ca as S/D electrodes. The improvement in device performance is due to improved electron injection at the interface, resulting from the narrowed and lowered tunneling barrier by the insertion of the Cs_2CO_3 layer. In addition, it also serves as a protective agent against unfavorable chemical reaction between the organic layer and the metal electrode. Further improvement of the device performance can be achieved by optimizing fabrication conditions.

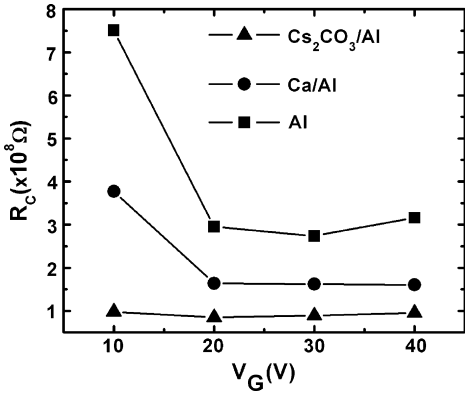

Fig. 3. Contact resistance vs. gate voltage for different materials as the source/drain contacts.

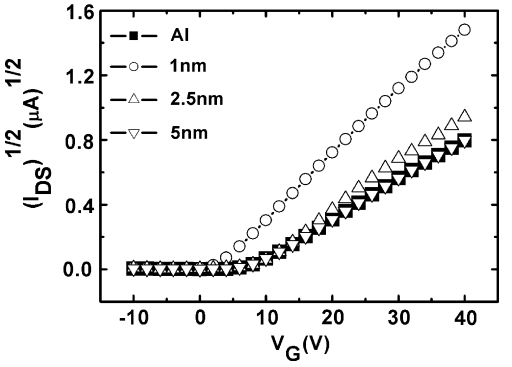

Fig. 4. $(I_{SD})^{1/2}$–V_G plots of OTFTs with a variety of Cs_2CO_3 thickness. Thicknesses of the Cs_2CO_3 layers are indicated.

Acknowledgements

Financial support from Academia Sinica, the National Science Council, ROC (NSC-95-2218-E-001-003) and the Ministry of Economic Affairs, ROC is deeply appreciated.

References

[1] P. Mach, S.J. Rodriguez, R. Nortrup, P. Wiltzius, J.A. Rogers, Appl. Phys. Lett. 78 (2001) 3592.
[2] B. Crone, A. Dodabalapur, Y.-Y. Lin, R.W. Filas, Z. Bao, A. LaDuca, R. Sarpeshkar, H.E. Katz, W. Li, Nature (London) 403 (2000) 521.
[3] P.F. Baude, D.A. Ender, M.A. Haase, T.W. Kelley, D.V. Muyres, S.D. Theiss, Appl. Phys. Lett. 82 (2002) 3964.
[4] Y. Lin, D.J. Gundlach, S.F. Nelson, T.N. Jackson, IEEE Trans. Electron Dev. 18 (1997) 606.
[5] S. Kobayashi, T. Takenobu, S. Mori, A. Fujiwara, Y. Iwasa, Appl. Phys. Lett. 82 (2003) 4581.
[6] T. Yasuda, T. Goto, K. Fujita, T. Tsutsui, Appl. Phys. Lett. 85 (2004) 2098.
[7] C. Waldauf, P. Schilinsky, M. Perisutti, J. Hauch, C.J. Brabec, Adv. Mater. 15 (2003) 2084.
[8] Th.B. Singh, N. Marjanović, G.J. Matt, N.S. Sariciftci, R. Schwödiauer, S. Bauer, Appl. Phys. Lett. 85 (2004) 5409.
[9] T.D. Anthopoulos, C. Tanase, S. Setayesh, E.J. Meijer, J.C. Hummelen, P.W.M. Blom, D.M. de Leeuw, Adv. Mater. 16 (2004) 2174.
[10] T.W. Lee, Y.H. Byun, B.W. Koo, I.N. Kang, Y.Y. lyu, C.H. Lee, L.S. Pu, S.Y. Lee, Adv. Mater. 17 (2005) 2180.
[11] X. Yan, J. Wang, H. Wang, H. Wang, D. Yan, Appl. Phys. Lett. 89 (2006) 053510.
[12] L.S. Hung, C.W. Tang, M.G. Mason, Appl. Phys. Lett. 70 (1997) 152.
[13] T. Hasegawa, S. Miura, T. Moriyama, T. Kimura, I. Takaya, Y. Osato, H. Mizutani, SID Int. Symp. Dig. Tech. Papers 35 (2004) 154.
[14] F.C. Chen, T.H. Chen, Y.S. Lin, Appl. Phys. Lett. 90 (2007) 073504.
[15] N.J. Watkins, L. Yan, Y.L. Gao, Appl. Phys. Lett. 80 (2002) 4384.
[16] J. Huang, G. Li, E. Wu, Q. Xu, Y. Yang, Adv. Mater. 18 (2006) 114.
[17] S.M. Sze, Physics of Semiconductor Devices, Wiley, New York, 1981.
[18] C.J. Brabec, N.S. Sariciftci, J.C. Hummelen, Adv. Funct. Mater. 11 (2001) 15.
[19] C.J. Brabec, A. Cravino, D. Meissner, N.S. Sariciftci, M.T. Rispens, L. Sanchez, J.C. Hummelen, T. Fromherz, Thin Solid Films 403–404 (2002) 368.
[20] C.I. Wu, C.T. Lin, Y.H. Chen, M.H. Chen, Y.J. Lu, C.C. Wu, Appl. Phys. Lett. 88 (2006) 152104.
[21] J.S. Huang, T. Watanabe, K. Ueno, Y. Yang, Adv. Mater. 19 (2007) 739.
[22] T.R. Briere, A.H. Sommer, J. Appl. Phys. 48 (1977) 3547.
[23] C.W. Chu, S.H. Li, C.W. Chen, V. Shrotriya, Y. Yang, Appl. Phys. Lett. 87 (2005) 193508.
[24] D.K. Schroder, Semiconductor material and device characterization, second ed., John Wiley & Sons, New York, 1998.
[25] L. Torsi, A. Dodabalapur, H.E. Katz, J. Appl. Phys. 78 (1995) 1088.
[26] Y. Li, D.Q. Zhang, L. Duan, R. Zhang, L.D. Wang, Y. Qiu, Appl. Phys. Lett. 90 (2007) 012119.
[27] S.T. Melnychuk, M. Seidl, J. Vac. Sci. Technol. A 9 (1991) 1650.